

FINITE ELEMENT MODELLING OF MULTIPLE COHESIVE DISCRETE CRACK PROPAGATION IN REINFORCED CONCRETE BEAMS (II): A CASE STUDY

Z.J. Yang
Department of Civil Engineering
Shantou University, Shantou
Guangdong 515063, PR China
(zyang1974@yahoo.com)

J. F. Chen^{*}
Institute for Infrastructure and Environment
Edinburgh University
The King's Buildings, Edinburgh EH9 3JN, UK
(J.F.Chen@ed.ac.uk)

Abstract

This paper presents a detailed case study using the finite element model for automatic simulation of multiple discrete crack propagation in reinforced concrete (RC) beams presented in the accompanying paper. A RC beam with well-documented test data is used in this study. The model is found capable of automatically modelling multiple crack propagation with high robustness, generality and efficiency. The predicted cracking process and distributed crack pattern are in close agreement with experimental observations. The load-deflection relations are accurately predicted up to a point when compressive cracking started to dominate. It is also found that the bond-slip properties can have significant effect on the predicted behaviour of the beam.

Keywords: Finite element analysis, local arc-length method, cohesive crack model, multiple crack propagation, reinforced concrete beam

Introduction

A finite element model for automatic simulation of multiple discrete crack propagation in reinforced concrete (RC) beams is presented in the companion paper [1]. This paper presents a detailed case study carried out using the model. The behaviour of a RC beam with well-documented test data is simulated. Numerical predictions of both cracking process and load-displacement relations are compared with experimental records. The effects of bond-slip modelling and the efficiency and effectiveness of the numerical algorithms, together with the limitations of the current model, are also discussed.

An example RC beam

Bresler and Scordelis carried out a series tests on RC beams [2]. Because the experiments were well controlled and detailed experimental data were published, they have since been widely used for validating nonlinear finite element models to simulate the behaviour of RC structures. For example, Cedolin and Dei Poli [3] modelled two of the test beams OA-1 and A-1. Barzegar and Maddipudi [4] also modelled the beam OA-1. Both studies used the smeared crack models. Test beam OA-2 was modelled in this study because its crack pattern at failure is available for comparison [2]. The beam was simply supported and subjected to a concentrated load at the mid-span.

^{*}Corresponding author. Tel. +44 131 650 6768; Fax. +44 131 650 6781
Email: J.F.Chen@ed.ac.uk

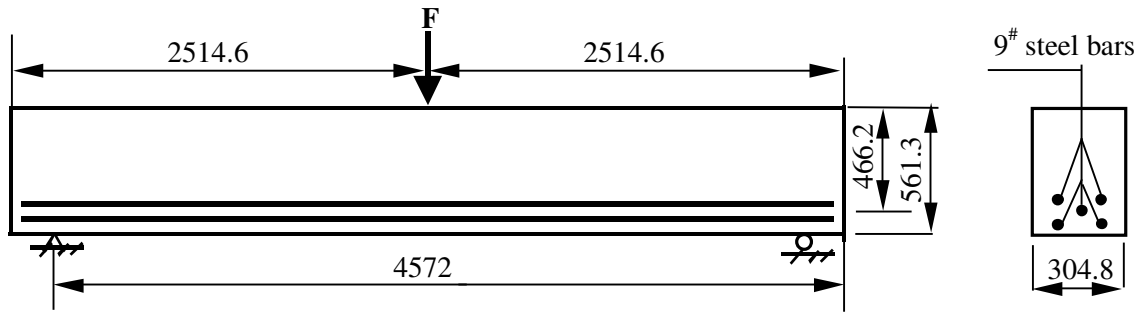


FIGURE. 1 RC beam OA-2 tested by Bresler and Scordelis [2] (unit: mm)

The test beam OA-2 had a length of 5.029m with a shear span of 4.572m (15ft) and a cross-section of 304.8×561.3mm (12×22.1in) (Fig.1). It was reinforced with five 9[#] high strength deformed steel bars with total nominal cross-sectional area of 3290mm² at an effective depth of 466.2mm. The beam was not reinforced with stirrups.

The concrete had a cylindrical compressive strength of $f'_c = 23.7\text{MPa}$ and the Young's modulus was evaluated from $E_c = 4730\sqrt{f'_c}$ to be 24GPa according to ACI 318-95 [5]. The tensile strength was evaluated from $f_t = 0.1f'_c = 2.37\text{MPa}$. For ordinary concrete, the fracture energy G_f has values between 65 and 200 N/m [6]. $G_f = 100\text{N/m}$ was used in this study. The parameters for Petersson's bilinear softening law (c.f. Fig. 2 in [1]) are thus: $\sigma_0 = f_t = 2.37\text{MPa}$, $w_c = 0.152\text{mm}$, $\sigma_1 = 0.79\text{MPa}$ and $w_1 = 0.034\text{mm}$. The value of w_0 is assumed as 0.0001mm with a high initial stiffness $k_0 = 2400\text{MPa/mm}$. The steel bars had a Young's modulus of 200 GPa and an average yield strength of 552MPa. The Poisson's ratios for the concrete and the steel bars were assumed here to be 0.18 and 0.3 respectively.

Finite element modelling

The reinforcing bars were modelled by two-node truss elements. The bulk of concrete was assumed to behave linear-elastically and modelled with four-node isoparametric and three-node constant strain elements. The cracks were modelled with four-node nonlinear interface elements. A plane stress condition was assumed for the analysis. Only half of the beam was modelled considering symmetry. Figure 2 shows an initial FE mesh for the example beam.

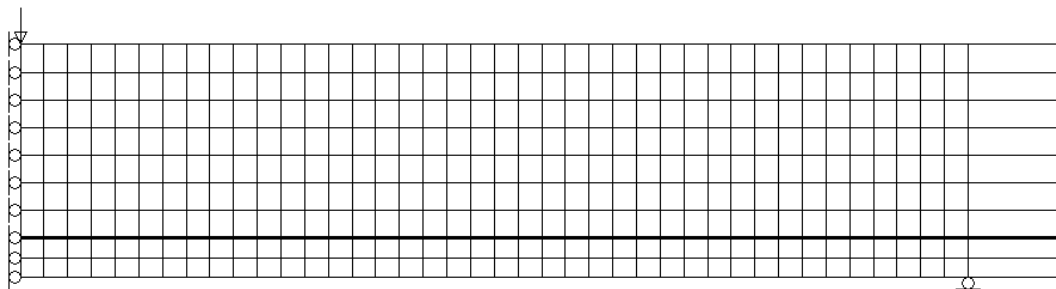


FIGURE.2 Initial finite element mesh: 410 elements and 420 nodes

The tension-softening elements described in [1] were used to model the bond-slip behaviour. The force-opening relation reported by Ingraffea et al [7] was slightly modified to consider the different steel yield strength (Fig. 3). In order to investigate the effect of bond-slip modelling on the simulation, two other relations were also modelled. One assumed a strong bond condition with a high constant stiffness (5400MPa/mm) whereas another assumed a weak bond with a much lower stiffness (1700MPa/mm) after the same initial stiffness. The three bond-slip relations are termed “Mild-Bond”, “Strong-Bond” and “Weak-Bond” hereafter for convenience of discussion.

The analysis was carried out according to Fig. 6 in [1]. Firstly, the nonlinear equation system at the current configuration was solved using the local arc-length algorithm. The crack initiation criterion and energy crack propagation criterion were then checked based on the converged stresses and displacements. Nonlinear interface elements were inserted at the nodes which satisfy the initiation criterion and the remeshing procedure was triggered at the existing crack tips where the energy crack propagation criterion is matched. The mesh mapping techniques were applied to transfer stresses and displacements to the new mesh, which was followed by another nonlinear analysis on the newly formed configuration. The iteration continued until the structure collapsed or some FE elements became too ill-shaped to result in accurate predictions.

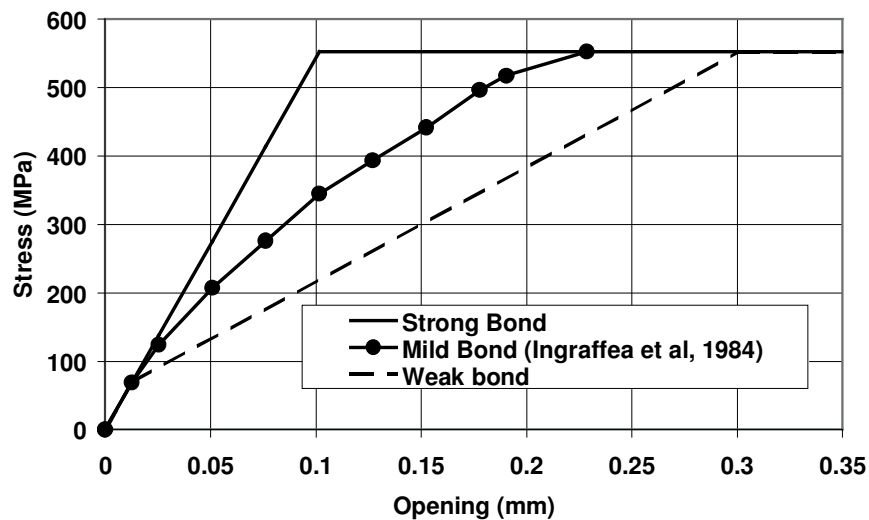


FIGURE.3 Bond-slip assumptions for tension-softening elements

Simulated results and discussion

Cracking process

Figures 4a-e illustrate the cracking process of the beam using the Strong-Bond data. A scale of 50 has been applied to the deformation for clarity of presentation. The dotted lines represent steel truss elements.

The FE simulation shows that a few flexural cracks first appear in the mid-span at a load about $F=60\text{KN}$ (Fig. 4a). As the load increases, these initial flexural cracks begin to propagate upwards with increasing crack widths. More cracks away from the mid-span are also initiated. At a load about 110KN (Fig. 4b), the major flexural cracks have propagated

into the upper half of the beam and the cracks become gradually curved towards the loading point. When the load is about 200KN (Fig. 4c), the major cracks have extended to about one third of the beam depth below the compression face. The widths of most cracks continue to increase steadily and more cracks are initiated away from the mid-span. The width of the cracks increase rapidly thereafter (Fig. 4d). The number of cracks has been stabilised by now. It is interesting to note that, as the load further increases (Fig. 4e), the crack width increases much faster in the mid-depth of the beam than at the level steel reinforcement because of the restraints of the reinforcing bars on the crack.

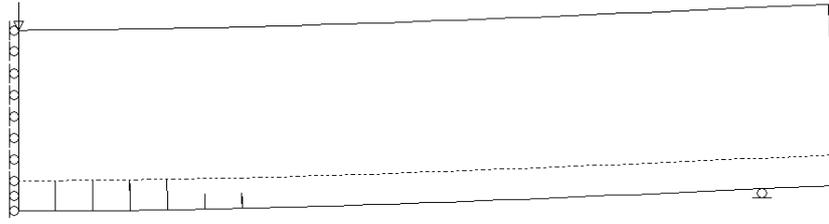
The analysis was terminated because some FE elements became too ill-conditioned due to remeshing. Although this remains a challenge to avoid such ill-conditioned meshes at late stage of analysis, this may become less a problem if the plastic behaviour concrete under compression is considered as discussed in the next section. It can be seen that the FE mesh has significantly changed in Figs 4a-e from the initial mesh (Fig. 2). The numbers of elements, nodes and interface elements increase from 410, 420 and 0 to 926, 696 and 115 respectively. It is remarkable that the adopted remeshing procedure can adapt such dramatic changes.

The predicted cracking process in general agrees well with experimental observations [2]. Figure 5a shows the test crack pattern [2], which may be compared with the predicted one as shown in Fig. 5b which is the same as Fig. 4d except that the un-deformed mesh is shown here. Within the shear span, the model predicted 16 cracks compared with 13 observed in test. It may be noted that the shear crack near the support is not modelled yet because in the current model only cracks on the tensile face of the beam are allowed to initiate and they are not allowed to propagate downwards to avoid remeshing difficulties. Further research is being carried out to alleviate these restrictions.

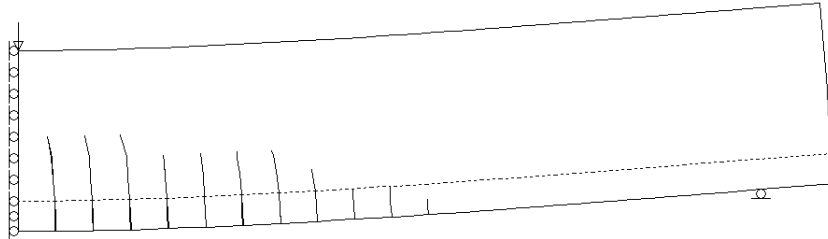
Load versus deflection and loading capacity

Figure 6 shows the predicted load versus deflection relationship at the mid-span using the Strong-Bond assumption. Test results from [2] are also shown for comparison. It can be seen that the prediction is in very close agreement with the test data for loading up to about 285KN. Beyond this point the stiffness of the beam is slightly over-predicted. This is inevitable because the plasticity of concrete under compression has not been considered in the current model.

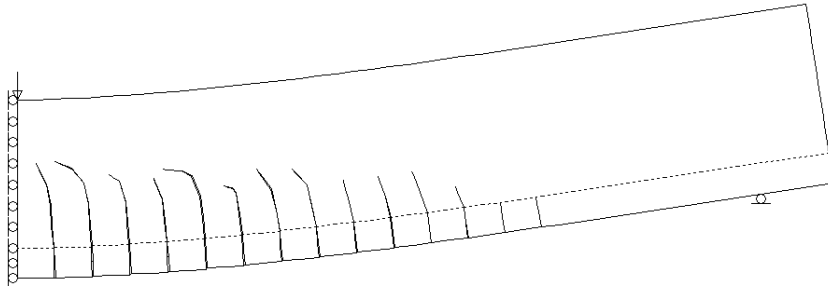
Figures 7a and b show contour of the principal compressive stress. $F=200\text{KN}$ (Fig. 7a), the compressive stress near the loading point has exceeded the concrete compressive strength ($f_c = 23.7\text{MPa}$) already. Because the plastic zone is confined to a very small zone at this stage even if it is considered, neglecting the plasticity has insignificant effect on the deflection. As the load is increased to $F=285\text{KN}$, the area where the principal compressive stresses exceeds f_c has expanded considerably. The actual plastic zone would be slightly larger than this area because of stress redistribution due to plastic deformation. The effect of plastic deformation of concrete on the stiffness of the beam thus starts to be visible.



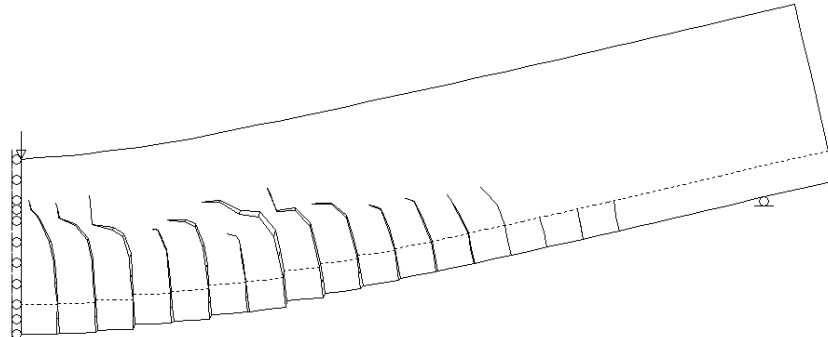
a) $F=73\text{KN}$, 484 nodes and 515 elements with 16 interface elements



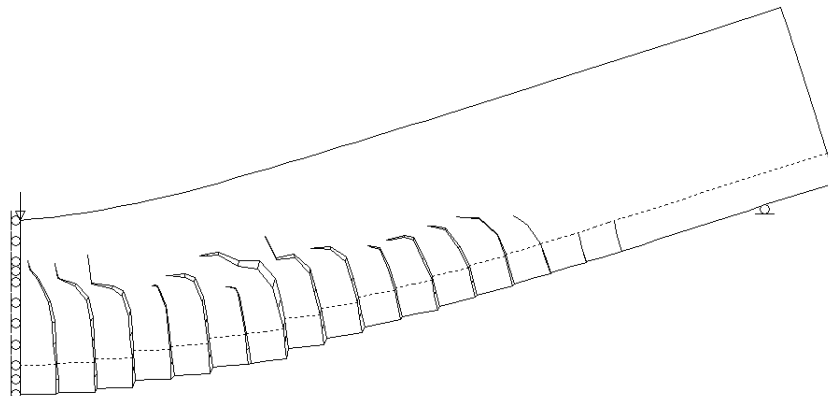
b) $F=115\text{KN}$, 552 nodes and 655 element with 51 interface elements



c) $F=200\text{KN}$, 618 nodes and 790 elements with 81 interface elements



d) $F=285\text{ KN}$, 693 nodes and 962 elements with 111 interface elements



e) $F=358\text{KN}$: 696 nodes and 926 elements with 115 interface elements

FIGURE.4 Simulated cracking process

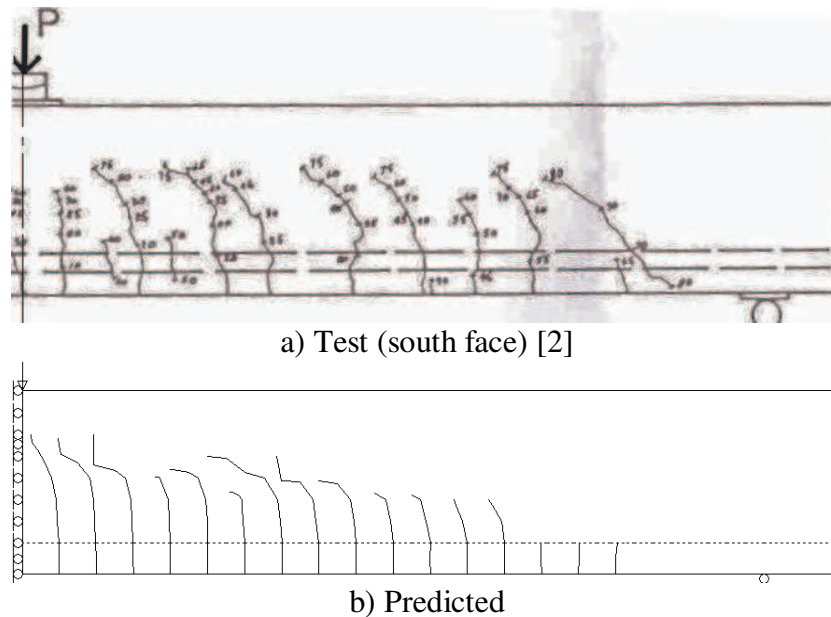


FIGURE.5 Crack pattern at failure

According to [2], a longitudinal splitting (compression cracks) started to occur in the compression zone near the loading point at a load about 80% (285KN) of the ultimate failure load (358KN) of the beam. “The failures occurred as a result of longitudinal splitting in the compression zone near the load point, and also by horizontal splitting along the tensile reinforcement near the end of the beam” [2]. The ultimate failure of the beam was due to the formation of a critical diagonal tension crack, joining a compressive splitting crack with a splitting crack at the reinforcement bar level.

The current discrete crack model cannot yet simulate this final failure process because neither the plasticity of the concrete under compression nor compression cracking is considered. Therefore, the predicted crack pattern (Fig. 4e) and load-deflection curve above $F=285\text{KN}$ (Fig. 6) do not accurately reflect the actual behaviour of the beam.

Further research is being undertaken to properly consider the plasticity of concrete under compression and concrete compression cracking, aiming at simulating the entire loading process of RC structures.

Effect of bond-slip modelling

All the three bond-slip assumptions as shown in Fig. 3 have been used to simulate the behaviour of the beam. The resulting cracking process and crack patterns are very similar in all three cases, but at a same loading level the crack widths predicted from using the Weak Bond are slightly larger than those from the other two bond-slip assumptions.

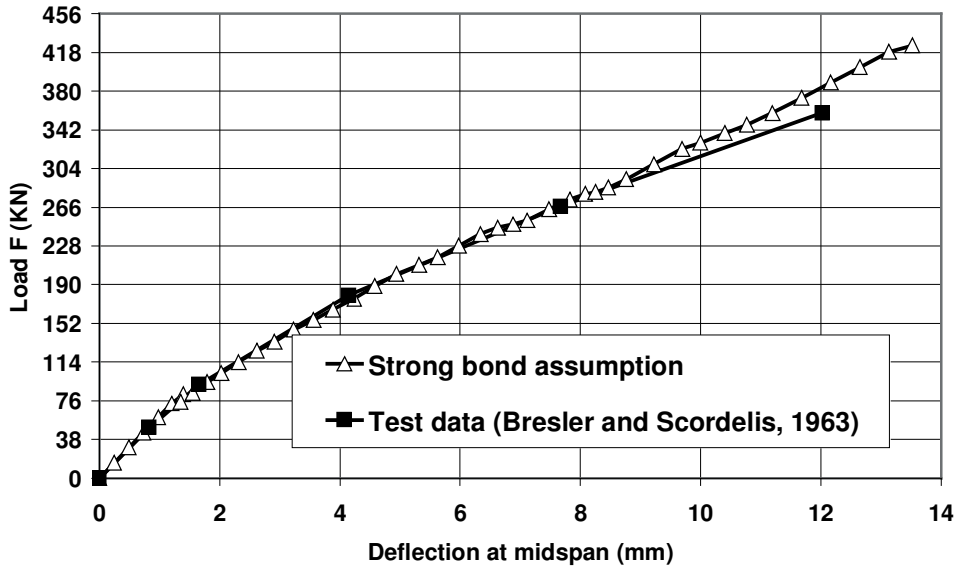
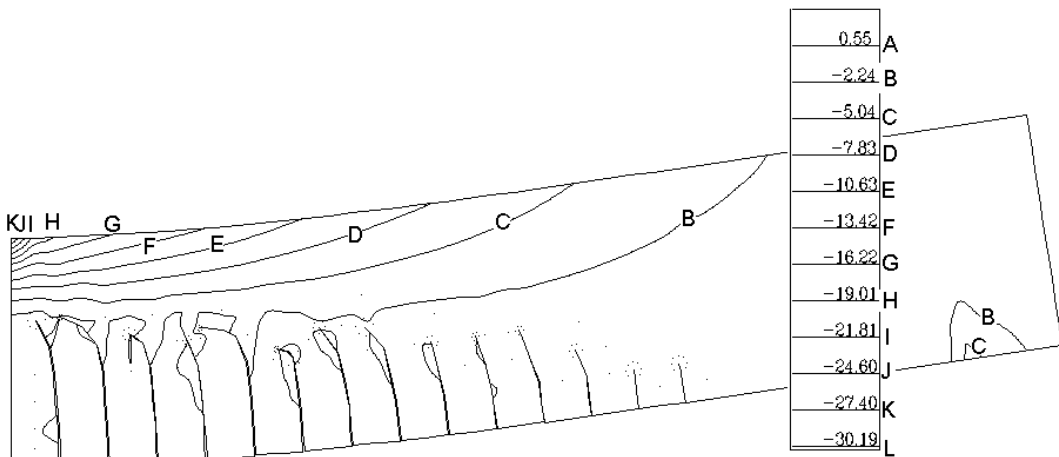
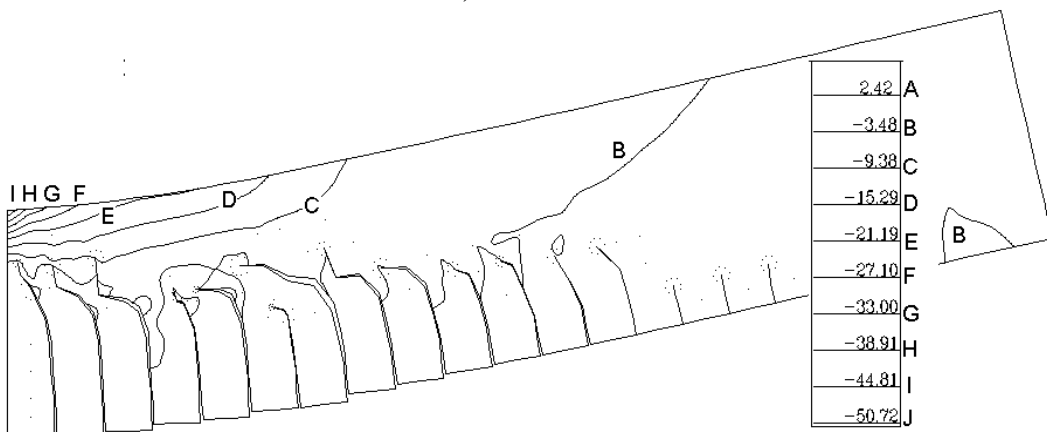


FIGURE.6 Predicted load-deflection curve using “strong bond” assumption



a) F=200kN



F=285kN

FIGURE.7 Contour of principal compressive stresses in concrete

Figure 8 shows the predicted load-deflection curves using the three bond-slip assumptions. All three curves are virtually identical up to a load about 110KN. This is understandable because at the initial cracking stage the cracks are still within the concrete cover or have just crossed the reinforcement bars. The effect of the bond-slip assumption does not take place yet if a crack is still within the concrete cover, or is still insignificant if the crack has just crossed the reinforcing bar.

Discrepancies between the Weak Bond model and the other two become significant when the load is above 160KN when the most of the cracks have penetrated a significant part of the beam depth. Because the significant lower stiffness of the tension-softening elements from the Weak Bond model allows the cracks to open more freely than the stronger bond-slip models, it considerably under predicts the stiffness of the beam. The Mild Bond assumption slightly under predicts the stiffness.

From this analysis, it may be concluded that the bond-slip between reinforcements and concrete has a significant effect on the overall structural behaviour of the beam. It also demonstrates that the two-node tension-stiffening element is able to model the bond-slip behaviour in an efficient and simple way, but further research is necessary to determine the accurate bond-slip relationship for the model.

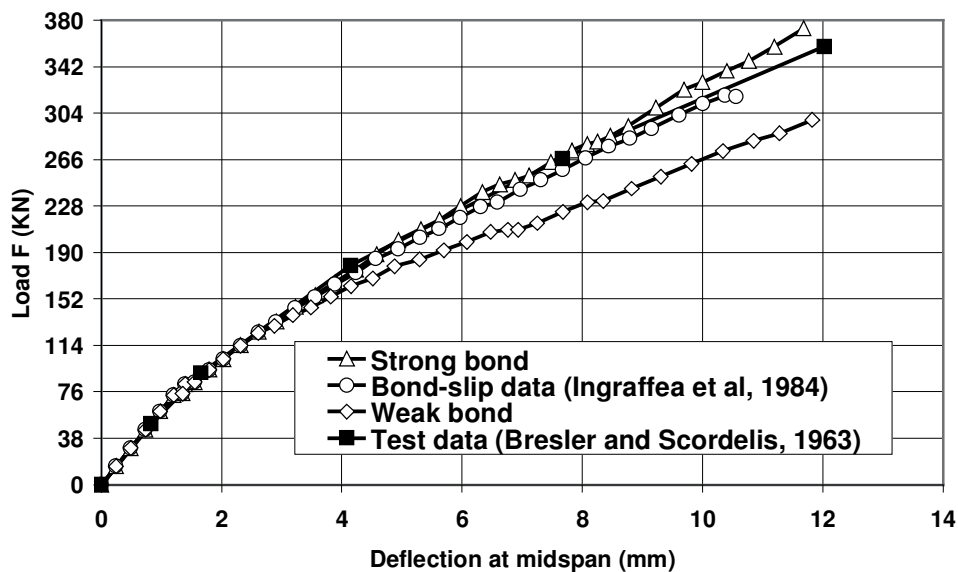


FIGURE.8 Effect of bond-slip assumption

Effectiveness of the local arc-length algorithm

Both tangential and secant iterative stiffness matrices for interface elements modelling the FPZ have been used with the local arc-length method to model the RC beam. The results show that although the tangential stiffness matrix based method is far more efficient than that based on secant stiffness matrix, it is less reliable than the latter and often leads to numerical instability and divergence, especially when a number of cracks initiate or propagate simultaneously. This may be due to its incompatibility with the unloading path assumed in the model (c.f. Fig. 2 in [1]), i.e., in one loading increment, the tangential stiffness at a Gauss point (Fig. 1 in [1]) may alter from negative on loading to positive on unloading and the vice

versa. In contrast, the secant stiffness is always positive during loading-unloading iterations, leading to better numerical convergence and stability. Another reason perhaps lies in the complexity of the multiple cracking problem such as the modelled RC beam. Some cracks in such a complex problem may experience opening-closure loops from one load increment to another. A previous study [8] showed that the tangential stiffness based arc-length algorithms succeeded in modelling a shear beam with a single crack which keeps opening during the whole loading process. Therefore, the use of secant iterative stiffness matrices is recommended.

Conclusion

The finite element model for automatic simulation of multiple discrete crack propagation in reinforced concrete (RC) beams, which has been presented in the companion paper [1], has been applied to simulate a RC beam with well-documented test data in this paper. The model was found capable of automatically modelling multiple crack propagation with high robustness, generality and efficiency. The predicted cracking process and distributed crack pattern agree well with experimental observations. The load-deflection relations are accurately predicted up to a point when compressive cracking becomes dominant. It has also been found that the bond-slip modelling has significant effect on the predicted behaviour of the beam. The limitations of the model are also briefly discussed, while further research is being carried out to address these issues.

Acknowledgement

The author would like to thank Dr. Ming Xie in Weidlinger Associate INC and Prof. Walter H. Gerstle in the Department of Civil Engineering of New Mexico University in the USA for their kind provision of program AUTOFRAP, a modified version of which has been incorporated into the program developed and used in this research.

Reference

- [1] Yang, Z.J. and Chen, J.F., *Proc., the 15th European Conference of Fracture*, Edited by Nilsson, F., KTH, Royal Institute of Technology, Sweden, August 11-13, 2004.
- [2] Bresler B. and Scordelis A.C., *J. ACI*, vol. 60, 51-74, 1963.
- [3] Cedolin L. and Del Poli S., *ASCE J. Engng. Mech Division*, vol. 103, 395-410, 1977.
- [4] Barzegar F. and Maddipudi S., *ASCE J. Struct. Engng.*, vol. 123, 1347-1356, 1995.
- [5] ACI 318-95., *Building Code Requirements for Structural Concrete (318-95) and Commentary (318R-95)*, American Concrete Institute, 1999.
- [6] Elfgren L., *Report of the technical committee 90-FMA fracture mechanics to concrete-applications*, RILEM, 1989, Chapman and Hall, London.
- [7] Ingraffea, A.R., Gerstle, W.H., Gergely, P. and Saouma, V., *ASCE J. Struct. Engng.*, vol. 110, 871-890, 1984.
- [8] Yang, Z.J. and Proverbs, D., *Engng. Fract. Mech.*, vol. 71, 81-105, 2003.